

# Manufacturing radar-absorbing composite materials by using magnetic Co-doped zinc oxide particles synthesized by Sol-Gel

Hüsnügül Yılmaz Atay<sup>1</sup>  and Öykü İçin<sup>2</sup>

Journal of Composite Materials  
2020, Vol. 54(26) 4059–4066  
© The Author(s) 2020  
Article reuse guidelines:  
sagepub.com/journals-permissions  
DOI: 10.1177/0021998320927754  
journals.sagepub.com/home/jcm



## Abstract

An indicator of being a strong country in today's world is that they have powerful weapons. In this sector where science is used exceedingly, the "stealth" takes an important place. Radar-absorbing materials are used in stealth technology to disguise an object from radar detection, such that it can allow a plane to be perceived as a bird. In this study, Co-doped zinc oxide reinforced styrofoam sheet composites were manufactured as radar-absorbing materials. For this purpose, Co-doped zinc–ZnO particles were synthesized via the Sol-Gel method with doping concentrations of 0%, 3%, 6%, 9%, and 12%. They were embedded in a styrofoam matrix with different loading levels to see the concentration dependence. The as-prepared powders were characterized by using X-ray diffraction and Scanning Electron Microscope-Energy Dispersive Spectroscopy. Magnetic characterization of samples was carried out using a vibrating sample magnetometer. Finally, the radar-absorbing test was applied with a network analyzer to achieve the main purpose of this research. It was concluded that Co-doped zinc oxide reinforced composites have electromagnetic properties that indicate potential applications in the radar-absorbing area.

## Keywords

Radar-absorbing materials, magnetic properties, zinc oxide, Co-doped, Sol-Gel

Date received: 19th January 2019; accepted: 27th April 2020

## Introduction

Electromagnetic pollution has risen with the rapid development of technology (electronic and telecommunications devices). Electromagnetic interference (EMI) adversely affects electronic devices working nearby, and also harms people.<sup>1,2</sup> Thus, researches focus on efficient microwave absorbing materials (MAMs) that have played a significant role in radar systems, satellite communications, wireless networks, and protection of living beings from the harmful action of electromagnetic waves.<sup>3–7</sup>

Radio detection and ranging system, radar, is basically an electromagnetic system used to detect the location and distance of an object from the point where it is placed. The mechanism is based on electromagnetic waves and calculations. When the radar waves hit an object, some portion is reflected, some is absorbed by the object, and some of this is returned to the radar set, where it is detected.<sup>8</sup> Essential information is calculated from this reflected energy such as the time taken for it

to be received, the strength of the returned signal, or the change in frequency of the signal. By minimizing or eliminating reflected signals, radar-absorbing materials are designed. Since some part of radar waves are not reversed, the radar provides a reduced signature for detecting absorbent materials, and this allows a plane to be perceived as a bird.<sup>9,10</sup>

Radar-absorbing materials differ in electromagnetic absorption performance. They carry product specifications for frequency range, surface resistivity, operating temperature, thickness, etc.<sup>11</sup> The phenomenon behind

<sup>1</sup>Department of Material Science and Engineering, İzmir Katip Çelebi University, Turkey

<sup>2</sup>Department of Materials Science and Engineering, İzmir Institute of Technology, Turkey

### Corresponding author:

Hüsnügül Yılmaz Atay, İzmir Katip Celebi Universitesi, Çiğli, İzmir 35620, Turkey.

Email: hgulyilmaz@gmail.com

the absorption is related to the complex permeability and permittivity which is considerably affected by various parameters. The type of materials, including composition and phases, is one of those parameters. The synthesis method is also important as it can affect the material properties. Layering is another important parameter, thus it could be a single layer or multi-layer coating. The understanding of all these parameters aids in the development of an efficient absorber design.<sup>12</sup> In this manner, by altering the dielectric and magnetic properties of existing material, a radar-absorbing material can be produced. Foams, plastics, and elastomers can be used for altering permittivity. Ferrites, iron, and cobalt–nickel alloys, which are magnetic materials, are used to change the permeability of the base materials.<sup>13</sup>

In recent years, different types of MAMs have been widely studied by researchers. These are carbon-based materials<sup>5</sup> (graphene and carbon nanotubes), ferromagnetic metals<sup>5</sup> and their composites (CoFe@Ti<sub>3</sub>C<sub>2</sub>T<sub>x</sub>,<sup>14</sup> Fe<sub>3</sub>O<sub>4</sub>@g-C<sub>3</sub>N<sub>4</sub>,<sup>15</sup> and NiCrAlY/Al<sub>2</sub>O<sub>3</sub>),<sup>16</sup> ceramic materials (BaTiO<sub>3</sub>, SiO<sub>2</sub>, SiC, and TiO<sub>2</sub>), wide bandgap semiconductors<sup>6</sup> (zinc oxide (ZnO)), metal–organic framework materials, and conducting polymer composites.<sup>1,6,7</sup> And also, according to their molding methods and working performance, MAMs can be prepared in various forms such as in the shape of bricks, paints or sheets, and thin films.<sup>17–19</sup> Such products are typically obtained through the application of one or more forms of absorbent fillers in a polymeric or rubber matrix.<sup>17,18</sup>

Among them, carbon-based MAMs have some drawbacks such as relatively lower conductivity, lower saturation magnetization, and lower permeability.<sup>5</sup> So, due to their magnetic performance, ferromagnetic metal particles (Fe, Ni, and Co), especially in nanoscale, are more attractive by researchers.

Lü et al. produced porous Co/C composites as microwave absorbing with maximum reflection loss (RL) of 35.3 dB, and the effective absorption bandwidth (RL ≤ 10 dB) of 5.80 GHz (8.40–14.20 GHz).<sup>5</sup>

On the other hand, ZnO and its hybrids were previously investigated as MAMs due to their attractive properties such as lightweight, semiconductive properties, and outstanding dielectric performance and also their low cost and large-scale synthesis.<sup>6,20</sup>

Modifying ZnO nanoparticles by doping with magnetic metals (Fe, Cobalt, Nickel) is an effective strategy for enhancing absorption efficiency. In a recent study, Fan et al.<sup>3</sup> synthesized hierarchical C/NiCo<sub>2</sub>O<sub>4</sub>/ZnO composites using the hydrothermal and Sol-Gel method that showed strong microwave absorbing performance with the minimum RL value of 43.61 dB at 11.61 GHz. And also, materials showed the absorption bandwidth RL ≤ 10 dB of 4.32 GHz (9.74–14.06 GHz).

As shielding materials for EMI, the synergistic effects of ZnO and reduced graphene oxide

(rGO)-coated wearable cotton fabrics were investigated in X-band (8.2–12.4 GHz). High absorption of ~90% was obtained with 3% by weight of rGO loaded with ZnO-coated cotton.<sup>1</sup>

Zhou et al.<sup>20</sup> prepared FeSiAl/ZnO-filled resin composite coatings for use in microwave absorption applications. The composite coating, which includes 35 wt% FeSiAl and 20 wt% ZnO powders, has microwave absorption performance with the absorption peak of –40.5 dB at 10.4 GHz and absorption band of 3.5 GHz in 8.6–12.1 GHz.

In this study, Co-doped ZnO was used as a magnetic material. For the last few years, the interest on ZnO has been increasing due to its remarkable physical properties and potential applications in various fields such as solar cells, diluted magnetic semiconductors, nanopiezotronics, UV detectors, chemical and gas sensors, etc.<sup>21</sup> ZnO is II–VI type binary semiconductor compound with a wide bandgap (3.37 eV) at room temperature. Thermodynamically, the hexagonal wurtzite phase of ZnO is stable at room temperature, in which each cation (Zn<sup>2+</sup>) is surrounded by four anions (O<sup>2-</sup>) at the corners of a tetrahedron.<sup>22</sup>

In recent years, the changing of properties of ZnO materials is a significant interest by researchers. Incorporation of transition metal ions into the material is one way of altering the properties of ZnO. The incorporation of transition metal ions may change the magnetism and conducting properties of the ZnO.<sup>23–26</sup> Concordantly, cobalt doping was performed to alter the magnetic properties of ZnO in the present work. For this purpose, Co-doped ZnO particles were synthesized via the Sol-Gel method with doping concentrations of 0%, 3%, 6%, 9%, and 12%. They were embedded in a polymeric matrix (styrofoam) with different loading levels. The as-prepared powders of Co-doped ZnO were characterized by using X-ray diffraction (XRD) and Scanning Electron Microscope (SEM)-Energy Dispersive Spectroscopy. Magnetic characterization of samples was carried out using a vibrating sample magnetometer (VSM). Finally, a radar-absorbing test was applied with a network analyzer.

## Materials and method

Co-doped ZnO powders were synthesized by the Sol-Gel method, briefly summarized in Figure 1. The used precursors are zinc acetate dihydrate (C<sub>4</sub>H<sub>6</sub>O<sub>4</sub>Zn·2H<sub>2</sub>O, Aldrich) and cobalt(II) acetate (CH<sub>3</sub>CO<sub>2</sub>)<sub>2</sub>Co, Aldrich), and a complexing agent is citric acid monohydrate (C<sub>6</sub>H<sub>8</sub>O<sub>7</sub>·H<sub>2</sub>O, Aldrich). The following compositions of Zn<sub>1-x</sub>Co<sub>x</sub>O, with  $x=0, 0.03, 0.06, 0.09,$  and  $0.12$  mol, were prepared. Zinc acetate and cobalt acetate were separately dissolved off in distilled water. The solution was mixed by magnetic stirrer until the transparent solution

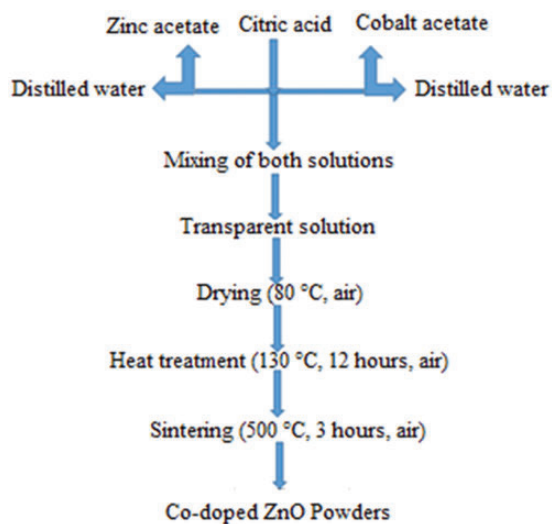


**Figure 1.** The flow chart for producing Co-doped ZnO powders.

was obtained. The solution was kept at 80 °C in the air until wet gel with high viscosity was obtained. The wet gel was treated at 130 °C for 12 h in the oven to prepare dry gel. The dry gel was exposed to the sintering process at 500 °C for 3 h to evaporate impurities and in the air in an ash furnace (Figure 1).

The phase analysis of powders was performed with the help of an Empyrean X-ray diffractometer with Cu K $\alpha$  radiation ( $\lambda = 1.540 \text{ \AA}$ ), in the  $2\theta$  range of 20–80°. SEM analysis was performed on Zeiss Sigma 300 VP-FESEM to study the morphology of powders. The room temperature magnetic behavior was evaluated by using VSM 550-100 VSM and polytetrafluoroethylene (PTFE) Teflon tape.

The electromagnetic parameters were measured with the transmission/reflection method in the region of 8–12 GHz with a Network Analyzer HP8720D. The network analyzer and coaxial line fixture have been calibrated. Obtained Co-doped ZnO powders were embedded between two styrofoam sheet blocks ( $22.86 \times 10.16 \times 2.0 \text{ mm}$ ). Prepared powders were laid as the layer between the two foams. The incident power is delivered by the network analyzer (Agilent 8720D model) with WR-90 waveguide. Then scattering parameters, reflection ( $S_{11}$ ) and transmission ( $S_{21}$ ), were measured.

## Results and discussions

Figure 2 shows XRD patterns of Co-doped ZnO powders ( $\text{Zn}_{1-x}\text{Co}_x\text{O}$ , with  $x = 0, 0.03, 0.06, 0.09,$  and  $0.12 \text{ mol}$ ) synthesized by Sol-Gel method. It revealed that all peaks corresponding to (100), (002), (101), (102), (103), (110), and (112) planes related to the hexagonal wurtzite crystal structure the wurtzite structure

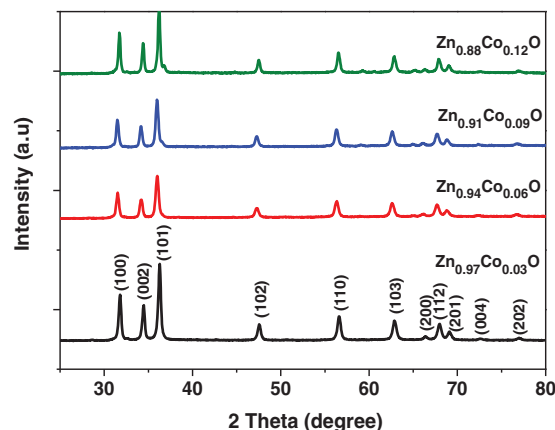


**Figure 2.** XRD patterns of Co-doped ZnO powders produced by the Sol-Gel method.

ZnO with Co-doped concentration up to 12%, in agreement with Joint Committee on Powder Diffraction Standards (JCPDS) card no: 89–0510.<sup>22,26</sup> There is no sign-related cobalt metal, oxides, or any binary zinc-iron phases. All the powders showed peaks similar to pure ZnO, which indicates that no structural deformation occurred in ZnO lattice upon Co-doping. This supports the successful substitutional replacement of Co ions in Zn lattice sites in the ZnO matrix.

Figure 3 depicts SEM micrographs of different doping concentration Co-doped ZnO powders. All samples have a spherical shape microstructure. The particle size of powders was measured via SEM. It can be said from the SEM micrographs, particle size distribution is around 120 nm. It is seen that the particles are agglomerated. The elemental composition of Co-doped ZnO was determined by Energy Dispersive X-Ray (EDX) analyses. Figure 4 shows the EDX spectra of Co-doped ZnO powders synthesized by the Sol-Gel method. The presence of Zn, O, and Co peaks are evident in the 3% (Figure 4(a)), 6% (Figure 4(b)), 9% (Figure 4(c)), and 12% (Figure 4(d)) Co-doped ZnO spectrum. EDX spectra show the presence of Zn, O, and Co element content in the powder, so conforming to the successful doping of Co atoms. The absence of other elements in the EDX spectrum affirms the phase-purity of the synthesized powders.<sup>27</sup>

The magnetization ( $M$ ) versus the applied magnetic field ( $H$ ) for  $\text{Zn}_{1-x}\text{Co}_x\text{O}$  ( $x = 0-12$ ) powders and different weight of  $\text{Zn}_{0.91}\text{Co}_{0.09}\text{O}$  powders at room temperature are shown in Figure 5. The magnetic properties of samples were measured by VSM measurements, putting into PTFE Teflon Tape. Room temperature ferromagnetism was observed for all the samples. Co-doped ZnO powders show high saturation magnetization as compared to un-doped ZnO. It is known that pure ZnO shows paramagnetic behavior, Co is the reason for the observed ferromagnetism in the Co-doped ZnO samples.<sup>28</sup> However, in this study, even undoped ZnO

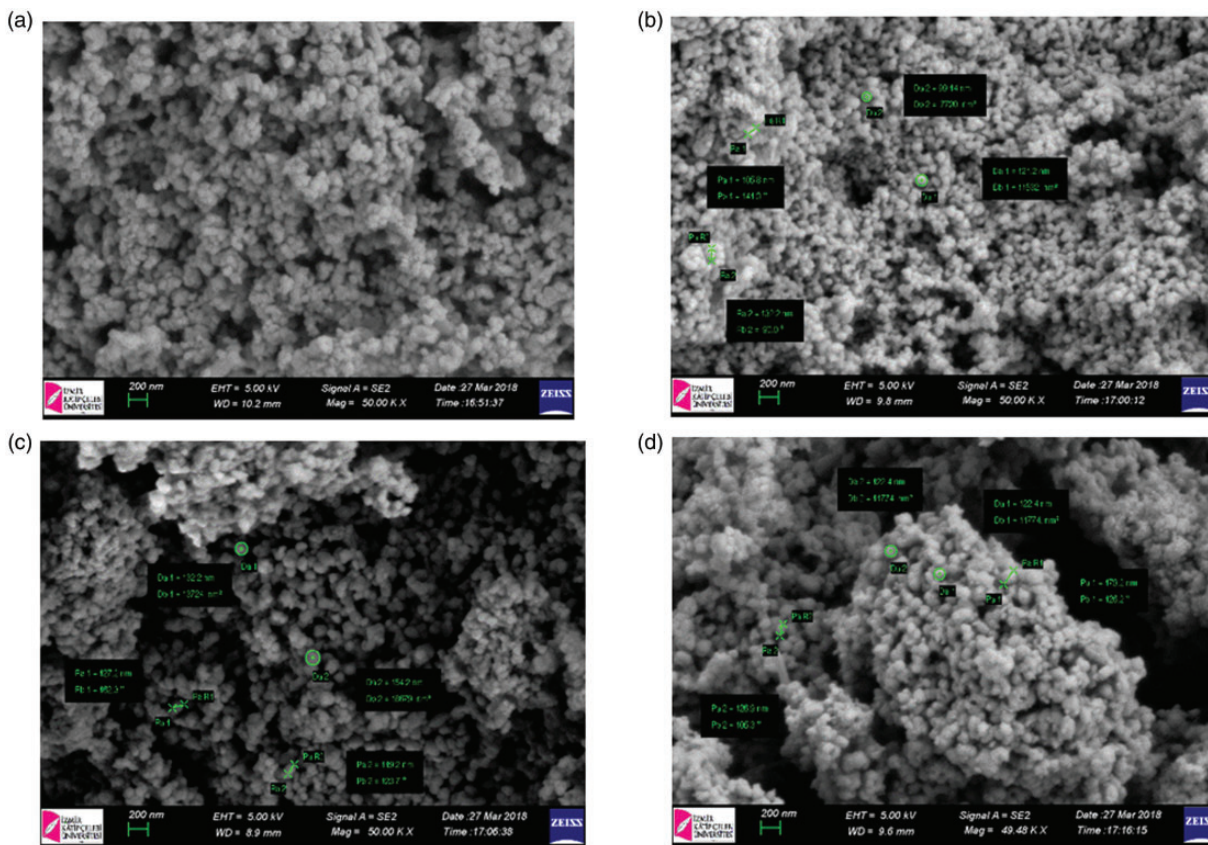


Figure 3. SEM micrographs of (a) 3%, (b) 6%, (c) 9%, and (d) 12% Co-doped ZnO powders.

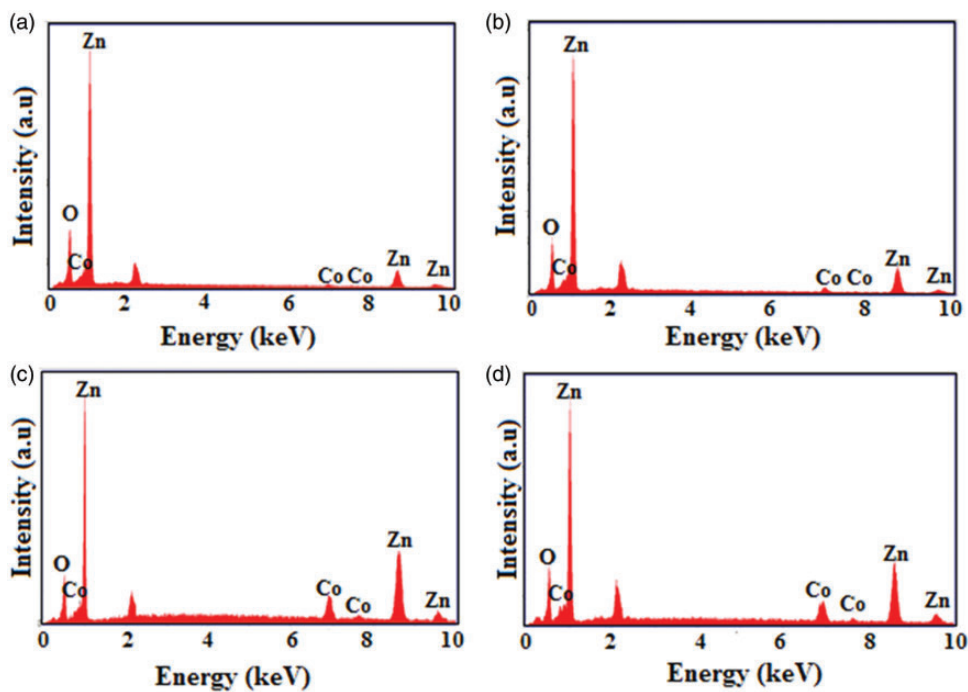


Figure 4. EDX spectrum of: (a) 3%, (b) 6%, (c) 9%, and 12% Co-doped ZnO powders.

powders showed ferromagnetic behavior. This effect comes about owing to the presence of oxygen vacancies that is the critical role of in appearance of the ferromagnetic phase has been proved in recent studies.<sup>29–31</sup> During the calcination process, the presence of carbon ions from precursor substances gives rise to the formation of oxygen vacancies in our samples.<sup>28,32</sup> In the case of doped diluted magnetic semiconductors, it can be

certain that the observed ferromagnetism in the  $Zn_{1-x}Co_xO$  powders originates from the Co substitution for Zn in ZnO. Another possible explanation is related to a nanoscale phase separation responsible for the presence of Co-rich magnetic nanoparticles.<sup>32</sup> Figure 5 shows that with increasing Co content from 0 to 0.12, saturation magnetization was increased from 0.035 to 0.12 emu/g, coercivity  $H_c$  is  $3.4 \times 10^4$  A/m, and loop area is  $18.1 \times 10^3$  Oe·emu/g.

The effect of the amount of Co-doped ZnO powders in Teflon composite is shown in Figure 5. The highest Co content ZnO powders ( $Zn_{0.91}Co_{0.09}O$ ) were used at different weight ratios in composite to compare the amount effects of these powders. With increasing weight ratios of 9% Co-doped ZnO powders in composite, saturation magnetization increased from 0.05 to 0.1.

To make the microwave absorption measurement, network analyzer and coaxial line fixture have been calibrated. Schematic presentation of the system is shown in Figure 6.

The incident power, the reflected ( $S_{11}$ ), and transmitted ( $S_{21}$ ) power were measured. The absorption ( $A$ ) was calculated by using the formula  $A (\%) = (1 - R - T) \times 100$ .<sup>1</sup> Figure 7(a) depicts microwave absorption characteristics of the pure styrofoam sheets block and Co-doped ZnO (3, 6, 9, and 12%) powder reinforced between styrofoam sheets block. It is clear to see in Figure 7, Co-doped ZnO powders reinforced composites showing significant absorbing activities. The radar wave absorbing properties of composites were substantially improved after the addition of Co-doped ZnO powders; absorbing percentage increases with increasing Co content in the powders.<sup>33–35</sup> The absorbing peak reaches 93% at 10.9 GHz with the 12% Co-doped ZnO powder reinforced composite. In Figure 7(b), 9% Co content ZnO powders ( $Zn_{0.91}Co_{0.09}O$ ) were used at a different amount in the composite. When the effect of the amount of the powders is compared, it is seen that

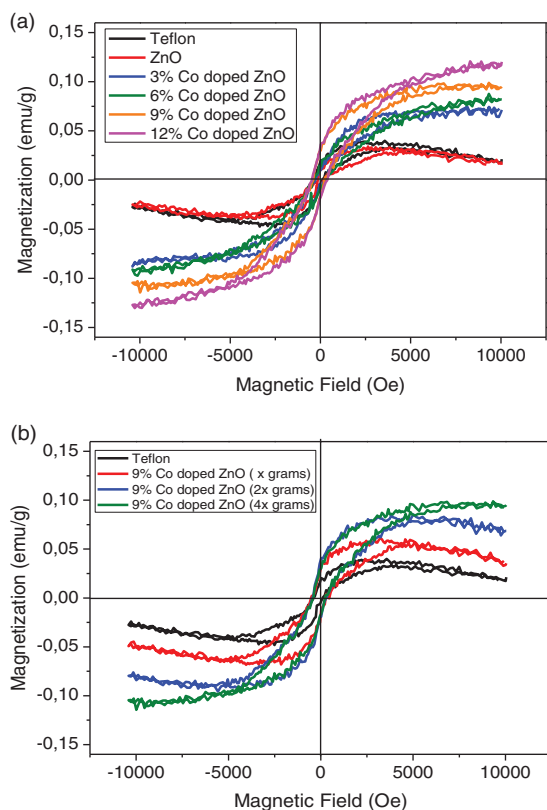


**Figure 5.** (a) M–H curves of  $Zn_{1-x}Co_xO$  and (b) different weight of  $Zn_{0.91}Co_{0.09}O$ .

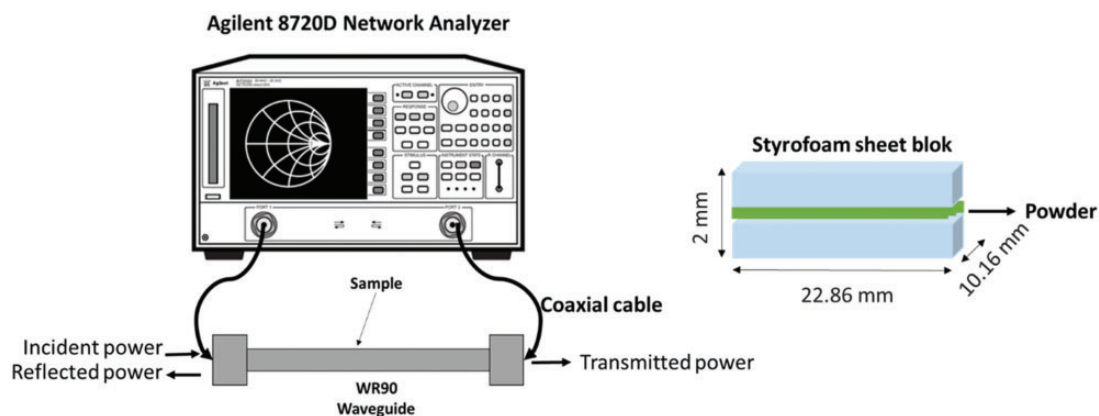


**Figure 6.** Schematic presentation of S-parameter measurement setup using 8720D network analyzer and prepared specimen.

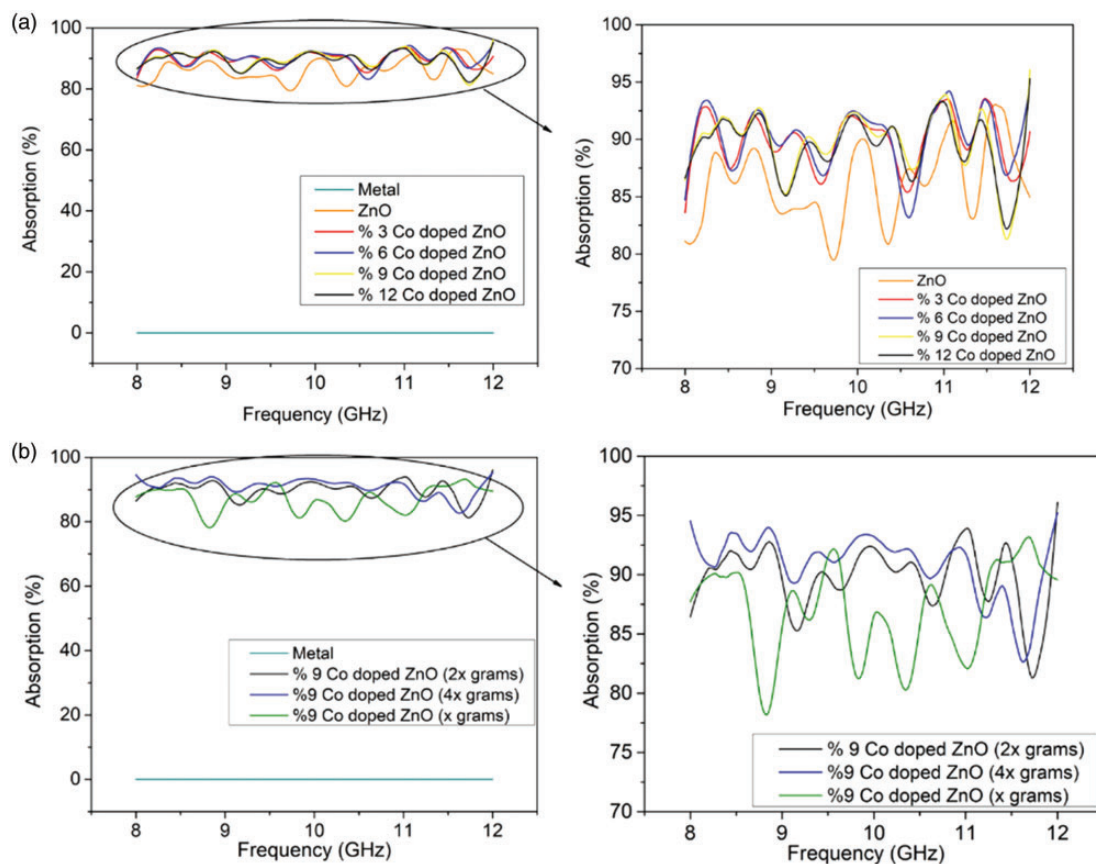


**Figure 7.** Absorption values (%) of (a)  $Zn_{1-x}Co_xO$  and (b) different weight of  $Zn_{0.91}Co_{0.09}O$ .

while  $x$  grams of 9% Co-doped ZnO powder reinforced composite has 90% absorption, the highest absorbing peak reaches 93.5% at 8.46 GHz with 4x grams of 9% Co-doped ZnO powder reinforced composite.<sup>10</sup>

The correlation between the measurements obtained by VSM and the network analyzer can be seen very clearly. When Co amount increased in the additive, the magnetization value increased. At the same time, radar absorption values also increased. Similarly, increasing the ZnO additive was shown to increase magnetization. In parallel, it was determined that this situation led to an improvement in radar absorption ability.

## Conclusion

Co-doped ZnO powders with the atomic fraction,  $x$ , in the range of 0–0.12 were successfully prepared by using a simple and economic Sol-Gel process. The effect of doping concentration on the structural and magnetic properties of Co-doped ZnO powders was studied. XRD results confirmed the presence of hexagonal wurtzite structure for all the synthesized samples and there are not any secondary phases. In SEM micrographs, it is seen that all samples have spherical

shape microstructure with an average around 120 nm of particle size. Also, EDX spectra results of samples prove that successful doping of Co atoms due to the presence of Zn, O, and Co element content in the powder. VSM results showed that room temperature ferromagnetic property enhanced with an increase in the doping concentration of cobalt. The observed ferromagnetism in the samples originates from the Co substitution for Zn–ZnO, which follows the electron double-exchange mechanism. The maximum saturation magnetization (0.12 emu/g) for the sample with a 12% doping concentration was obtained. Any absorbing activity in 0% additive content composite was not seen. However, in the highest loading level of (12%) Co-doped ZnO powders reinforced styrofoam sheets, there was significant absorbing activity. Absorption values were increased by increasing the content of Co in the ZnO powders, and also by increasing additive content between styrofoam sheets.

## Declaration of Conflicting Interests

The author(s) declared no potential conflicts of interest with respect to the research, authorship, and/or publication of this article.

## Funding

The author(s) received no financial support for the research, authorship, and/or publication of this article.

## ORCID iD

Hüsnügül Yılmaz Atay  <https://orcid.org/0000-0002-4291-4703>

## References

1. Gupta S, Chang C, Anbalagan AK, et al. Reduced graphene oxide/zinc oxide coated wearable electrically conductive cotton textile for high microwave absorption. *Compos Sci Technol* 2020; 188: 107994.
2. Sun J, Wang L, Yang Q, et al. Preparation of copper-cobalt-nickel ferrite/graphene oxide/polyaniline composite and its applications in microwave absorption coating. *Prog Org Coat* 2020; 141: 105552.
3. Fan J, Xing W, Huang Y, et al. Facile fabrication hierarchical urchin-like C/NiCo<sub>2</sub>O<sub>4</sub>/ZnO composites as excellent microwave absorbers. *J Alloys Compd* 2020; 821: 153491.
4. Jafarian M, Afghahi SSS, Atassi Y, et al. New insights on microwave absorption characteristics of magnetodielectric powders: effect of matrix chemical nature and loading percentage. *J Magn Magn Mater* 2019; 492: 165624.
5. Zhao X, Guo D-M, An Q-D, et al. Hierarchical nitrogen/cobalt co-doped carbonaceous materials with electromagnetic waves absorption promoting nanostructures. *J Alloys Compd* 2020; 822: 153666.
6. Luo J, Zhang K, Cheng M, et al. MoS<sub>2</sub> spheres decorated on hollow porous ZnO microspheres with strong wide-band microwave absorption. *Chem Eng J* 2020; 380: 122625.
7. Deng Z, He S, Wang W, et al. Construction of hierarchical SnO<sub>2</sub>@ Fe<sub>3</sub>O<sub>4</sub> nanostructures for efficient microwave absorption. *J Magn Magn Mater* 2020; 498: 166224.
8. Trujillo A and Thurman H. The black arts: materials and process selection and stealth technology. *Essent Oceanogr* 2004; 4: 36–45.
9. Varshney L. *Radar principles*. Revision: 3. Syracuse, NY: Syracuse Research Corporation, 2002.
10. Atay HY and Çelik E. Barium hexaferrite reinforced polymeric dye composite coatings for radar absorbing applications. *Polym Compos* 2014; 35: 602–610.
11. Ali I and Gupta V. Advances in water treatment by adsorption technology. *Nat Protoc* 2006; 1: 2661.
12. Kumar A and Singh S. Development of coatings for radar absorbing materials at X-band. *IOP Conf Ser: Mater Sci Eng* 2018; 330: 012006.
13. Kojima H. Fundamental properties of hexagonal ferrites with magnetoplumbite structure. *Handb Ferromagn Mater* 1982; 3: 305–391.
14. Zhou C, Wang X, Luo H, et al. Interfacial design of sandwich-like CoFe@ Ti<sub>3</sub>C<sub>2</sub>T<sub>x</sub> composites as high efficient microwave absorption materials. *Appl Surf Sci* 2019; 494: 540–550.
15. Yu J, Chi F, Sun Y, et al. Assembled porous Fe<sub>3</sub>O<sub>4</sub>@ g-C<sub>3</sub>N<sub>4</sub> hybrid nanocomposites with multiple interface polarization for stable microwave absorption. *Ceram Int* 2018; 44: 19207–19216.
16. Zhou L, Su G, Wang H, et al. Influence of NiCrAlY content on dielectric and microwave absorption properties of NiCrAlY/Al<sub>2</sub>O<sub>3</sub> composite coatings. *J Alloys Compd* 2019; 777: 478–484.
17. Anh LTQ and Van Dan N. A microwave-absorbing property of super-paramagnetic zinc-nickel ferrite nanoparticles in the frequency range of 8–12 GHz. *Appl Phys A* 2020; 126: 1–6.
18. Folgueras LdC, Alves MA and Rezende MC. Microwave absorbing paints and sheets based on carbonyl iron and polyaniline: measurement and simulation of their properties. *J Aerosp Technol Manag* 2010; 2: 63–70.
19. Shao T, Ma H, Feng M, et al. A thin dielectric ceramic coating with good absorbing properties composed by tungsten carbide and alumina. *J Alloys Compd* 2020; 818: 152851.
20. Zhou L, Yu J, Chen M, et al. Influence of particle size on the microwave absorption properties of FeSiAl/ZnO-filled resin composite coatings. *J Mater Sci Mater Electron* 2020; 31: 1–8.
21. Fabbiyola S, Kennedy LJ, Aruldoss U, et al. Synthesis of Co-doped ZnO nanoparticles via co-precipitation: structural, optical and magnetic properties. *Powder Technol* 2015; 286: 757–765.
22. Srinivasulu T, Saritha K and Reddy KR. Synthesis and characterization of Fe-doped ZnO thin films deposited by chemical spray pyrolysis. *Mod Electron Mater* 2017; 3: 76–85.
23. Franco A Jr, Pessoni H, Ribeiro P, et al. Magnetic properties of Co-doped ZnO nanoparticles. *J Magn Magn Mater* 2017; 426: 347–350.
24. Norberg NS, Kittilstved KR, Amonette JE, et al. Synthesis of colloidal Mn<sup>2+</sup>: ZnO quantum dots and high-TC ferromagnetic nanocrystalline thin films. *J Am Chem Soc* 2004; 126: 9387–9398.
25. Garcia MA, Merino JM, Fernández Pínel E, et al. Magnetic properties of ZnO nanoparticles. *Nano Lett* 2007; 7: 1489–1494.
26. Hammad TM, Griesing S, Wotocek M, et al. Optical and magnetic properties of Fe-doped ZnO nanoparticles prepared by the sol-gel method. *Int J Nanopart* 2013; 6: 324–337.
27. Vijayalakshmi K and Sivaraj D. Enhanced antibacterial activity of Cr doped ZnO nanorods synthesized using microwave processing. *RSC Adv* 2015; 5: 68461–68469.
28. Baranowska-Korczyn A, Reszka A, Sobczak K, et al. Magnetic Fe doped ZnO nanofibers obtained by electrospinning. *J Sol-Gel Sci Technol* 2012; 61: 494–500.
29. Cheng W and Ma X. Structural, optical and magnetic properties of Fe-doped ZnO. *J Phys Conf Ser* 2009; 152: 012039.
30. Samariya A, Singhal R, Kumar S, et al. Defect-induced reversible ferromagnetism in Fe-doped ZnO semiconductor: an electronic structure and magnetization study. *Mater Chem Phys* 2010; 123: 678–684.
31. Ashraf R, Riaz S, Kayani ZN, et al. Structural and magnetic properties of iron doped ZnO nanoparticles. *Mater Today Proc* 2015; 2: 5384–5389.

32. Bonanni A and Dietl T. A story of high-temperature ferromagnetism in semiconductors. *Chem Soc Rev* 2010; 39: 528–539.
33. Atay HY and Çelik E. Multifunctional polymer composites: antibacterial, flame retardant, radar absorbing and self-healing. *J Compos Mater* 2015; 49: 2469–2482.
34. Silva VA and Rezende MC. Effect of the morphology and structure on the microwave absorbing properties of multiwalled carbon nanotube filled epoxy resin nanocomposites. *Mater Res* 2018; 21: 72–75.
35. Pinto SS, Machado JPB, Gomes NAS, et al. The influence of morphology, structure, and weight fraction of magnetic additives on the electromagnetic characteristics of composites. *J Magn Magn Mater* 2019; 484: 126–138.